INTERNATIONAL JOURNAL FOR NUMERICAL METHODS IN FLUIDS
Int. J. Numer. Meth. Fluids **28**: 663–677 (1998)

A FINITE VOLUME METHOD FOR FLUID FLOW IN POLAR CYLINDRICAL GRIDS

L. MA, D.B. INGHAM* AND X. WEN

Department of Applied Mathematical Studies, The University of Leeds, Leeds LS2 9JT, UK

SUMMARY

In the numerical simulation of fluid flows using a polar cylindrical grid, grid lines meet at a single point on the axis of the polar cylindrical grid system; this makes the grids around the axis degenerate from being general quadrilaterals into triangles. Therefore, a special treatment must be performed when the axis has to be included in the computational domain in order to solve a non-axisymmetrical fluid flow problem. In this paper a new numerical method has been developed to deal with the difficulty of the axis when the control volume technique is used with a non-staggered grid arrangement. Two illustrative examples of the proposed method are presented for simulating the fluid flows on the axis and all the numerical results obtained for the two examples are shown to be in good agreement with the available analytical solutions. © 1998 John Wiley & Sons, Ltd.

KEY WORDS: CFD; control volume; polar cylindrical grid

1. INTRODUCTION

Due to the rapid development of the computational fluid dynamics (CFD) technique in the past decades, a great number of fluid flows in scientific and engineering applications can now be simulated quite satisfactorily by using the control volume CFD technique; especially when the geometrical boundary of the fluid flow to be simulated is regular and where a Cartesian grid system has been employed. When the simulated fluid flow has a curved boundary, more accurate results may be obtained by using a body fitted grid system to represent the curved fluid flow boundary. However, when the simulated fluid flow, or the geometry of the problem, has a cylindrical feature, e.g. when simulating the fluid flow in a curved pipe, a circular jet flow, etc., a polar cylindrical grid system, or more generally the so called O-type grid system, is often preferred [1].

However, when a polar cylindrical grid system, or the O-type grid system, is employed for the finite-volume method, grid lines meet at a single point on the axis where $r = 0$ and the cells around the axis degenerate from being general quadrilateral cells to triangular cells [2]. Therefore, a special treatment must be performed on the axis in order to solve a non-axisymmetrical fluid flow problem when the axis has to be included in the computational domain.

One of the simplest and most popular ways of avoiding this problem of the axis, which may be encountered when using the polar cylindrical grid, is to use a Cartesian grid system, even though the region to be simulated may be a circular cylinder; see Figure 1 for an example of

* Correspondence to: Department of Applied Mathematical Studies, The University of Leeds, Leeds LS2 9JT, UK.

CCC 0271–2091/98/140663–15$17.50
© 1998 John Wiley & Sons, Ltd.
Received June 1997
Revised September 1997

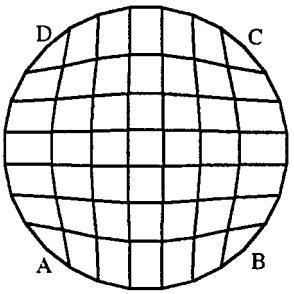

Figure 1. A typical Cartesian grid system when used in a circular region.

such a grid arrangement. In this grid system, cells near to the points A–D are highly deformed and the grid lines are greatly distorted from being orthogonal; this is undesirable as it may result in an overall deterioration in the accuracy of the simulation. Another method for dealing with the axis of the polar cylindrical grid is to employ a mixed Cartesian and cylindrical grid system, i.e. use a Cartesian grid system in the region near the axis and a cylindrical grid system in the region away from the axis, see Figure 2. In the previous attempts at dealing with the axis when the polar cylindrical grid system is retained, some authors have made certain simplifications, or introduced special variables for their specific problem, in order to evaluate the fluid flow quantities on the axis [3], other authors have used extrapolations or averages to compute the fluid flow quantities on the axis [4], but this may cause a reduction in the overall computational accuracy of the numerical scheme in some fluid flow simulations. Because of the difficulties encountered in the treatment of the axis of the polar cylindrical grid system, very few research papers have been published using a polar cylindrical grid, in which the fluid flows across the axis and no general treatment of the axis has, as yet, been published.

In this paper a new numerical method for dealing with the axis has been developed by using a circular control volume cell on the axis, Figure 3, for the purpose of solving general three-dimensional non-axisymmetrical fluid flow problems in a polar cylindrical grid system, or in any of the O-type grid systems. In this paper, a two-dimensional presentation of the proposed new method will be made in a polar cylindrical grid system and the extension of the method to more complicated three-dimensional cases is discussed.

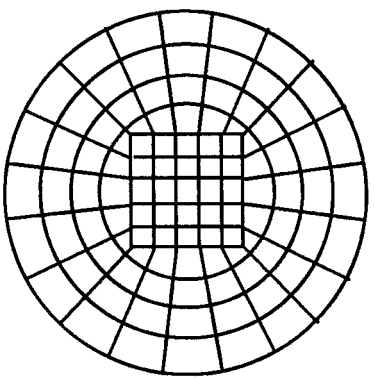

Figure 2. A mixed Cartesian and polar cylindrical grid system used in a circular region.

© 1998 John Wiley & Sons, Ltd.

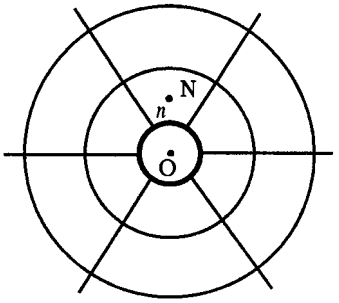

Figure 3. The control volume used on the axis of the polar cylindrical grid system.

In order to illustrate the technique, two simple, two-dimensional test examples have been presented. They are the numerical solutions of (a) the solid body rotating fluid flow inside a two-dimensional circular cylinder that is produced by the steady rotation of the cylinder, and (b) the fully developed fluid flow in a two-dimensional channel by using the control volume technique [5] with a non-staggered grid arrangement [6]. The numerical results for both of the fluid flows have been compared with the analytical solutions that can easily be obtained for these simple fluid flows.

2. GOVERNING EQUATIONS

For steady, incompressible fluid flow, the Navier–Stokes and continuity equations may be written in vector form as

$$\nabla\cdot(\rho\mathbf{V}\mathbf{V}) = -\nabla p + \nabla\cdot(\mu\nabla\mathbf{V}) \tag{1}$$

and

$$\nabla\cdot(\rho\mathbf{V}) = 0, \tag{2}$$

respectively, where ρ is the fluid density, μ is the fluid viscosity, p is the fluid pressure and $\mathbf{V}$ is the fluid velocity. When the Cartesian velocity components are employed, the momentum Equation (1) may be further written as

$$\nabla\cdot(\rho\mathbf{V}u_i) = -\frac{\partial p}{\partial x_i} + \nabla\cdot(\mu\nabla u_i), \tag{3}$$

where u_i is the i-direction component of the fluid velocity in a Cartesian co-ordinate system.

2.1. Discretized governing equations in a polar cylindrical grid system

For a typical polar cylindrical grid system, which is shown in Figure 4 for a two-dimensional case, if we integrate the momentum Equation (3) over the control volume P in the computational domain and using the Divergence Theorem, Equation (3) becomes

$$\sum_{nn}(\rho\mathbf{V}\cdot\mathbf{A}u_i)_{nn} - \sum_{nn}(\mu\nabla u_i\cdot\mathbf{A})_{nn} = -\Omega\left(\frac{\partial p}{\partial x_i}\right)_{\mathrm{P}}, \tag{4}$$

where $\mathbf{A}$ and Ω are the face area vector and the volume of the control volume P, respectively, and the subscript nn stands for the face of the control volume which takes the value e, w, n or s, see Figure 4. Equation (4) may be further written as the following discretized equation

© 1998 John Wiley & Sons, Ltd.

$$a_{\mathrm{P}}u_{i,\mathrm{P}} = \sum_{nb} a_{nb}u_{i,nb} - \Omega\left(\frac{\partial p}{\partial x_i}\right)_{\mathrm{P}} + s_Q, \tag{5}$$

where s_Q is a source term produced when the QUICK scheme [7] is employed and the a's are the coefficients representing the effects of convection and diffusion, and may be given by the upwind scheme as

$$a_e = D_e + [-F_e, 0], \qquad a_w = D_w + [F_w, 0], \tag{6}$$

$$a_n = D_n + [-F_n, 0], \qquad a_s = D_s + [F_s, 0], \tag{7}$$

and

$$a_{\mathrm{P}} = \sum_{nb} a_{nb}, \tag{8}$$

where the subscript nb denotes the neighboring cells of the cell P, including the east (E), west (W), north (N) and the south (S) cells.

The SIMPLE pressure–velocity coupling algorithm [5] is used to compute the fluid pressure, and this gives rise to a pressure correction equation from the continuity equation as follows

$$a'_{\mathrm{P}}p'_{\mathrm{P}} = \sum_{nb} a'_{nb}p'_{nb} + F_e - F_w + F_n - F_s, \tag{9}$$

where F is the mass flux of the fluid through the faces of the control volume and it may be calculated by using the pressure smoothing technique [6] which has been developed for the non-staggered grid system, p' is the pressure correction, and the a's are the coefficients which can be defined by

$$a'_{\mathrm{P}} = \sum_{nb} a'_{nb} \quad \text{and} \quad a'_{nn} = \rho_{nn}A^2_{nn}/\bar{a}_{nn}, \tag{10}$$

where $\bar{a}_{nn}$ is an average of the coefficients a_{P} in Equation (5) between two adjacent cells. For more details of the derivation of the Equations (5)–(10) refer to References [5,6].

3. DISCRETIZED GOVERNING EQUATIONS ON THE AXIS OF A POLAR CYLINDRICAL GRID SYSTEM

3.1. Control volume on the axis

For a polar cylindrical computational domain that does not include the axis in the solution domain, there are no difficulties in computing the fluid pressures and the velocities by solving

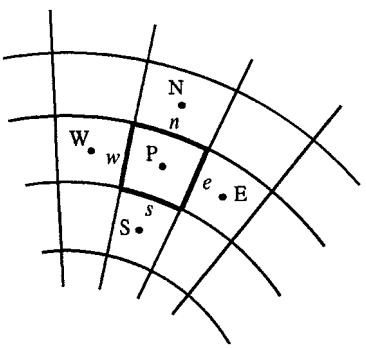

Figure 4. A typical polar cylindrical grid.

© 1998 John Wiley & Sons, Ltd.

the discretized Equations (5) and (9) using an iterative strategy. However, when the axis is included in the computational domain for a non-axisymetrical fluid flow simulation, difficulties may be encountered when applying Equations (5) and (9) on the cells around the axis where triangular cells exist.

In order to eliminate the difficulties which occur on the axis due to the degeneration of the grid shape, from being a general quadrilateral to being triangular, under the general polar cylindrical grid system, we employ a circular cell, or to be more precise a polygon, on the axis in order to replace the triangular cells around the axis, see Figure 3. The circular cell on the axis is formed by joining all the triangular cells around the axis and all the fluid flow variables for the circular cell are stored on the axis.

3.2. Discretized momentum equations on the axis

In order to obtain a discretized form of the momentum equation on the axis, by integrating the momentum Equation (3) over the circular cell on the axis, see Figure 3, and using the Divergence Theorem we obtain the following equation

$$\sum_n (\rho \mathbf{V} \cdot \mathbf{A} u_i)_n - \sum_n (\mu \nabla u_i \cdot \mathbf{A})_n = -\Omega \left(\frac{\partial p}{\partial x_i} \right)_O, \tag{11}$$

where the subscript n denotes the value of the fluid flow quantity on the face segment of the circular cell which corresponds to each general polar cylindrical cell next to the circular cell, the subscript O is the axis, see Figure 3, and the vector $\mathbf{A}$ is the outward normal area vector to the face of the circular cell on the axis. As we can see, Equation (11) has a similar form to that of Equation (4) but different ways are used to compute each term in these equations.

In order to compute the fluid diffusion term, $\nabla u_i \cdot \mathbf{A}$, on the face of the circular control volume, virtually only the radial component of the fluid velocity gradient ∇u_i is needed and this can be computed using the central-difference scheme as follows

$$(\nabla u_i \cdot \mathbf{A})_n = (u_{i,N} - u_{i,O}) A_n / r_N, \tag{12}$$

where r_N is the radial distance of the cell center N from the axis.

The pressure gradient source term on the right-hand side of Equation (11) may be computed by using the pressure on the face of the circular cel1 and it may be expressed as

$$-\Omega \left(\frac{\partial p}{\partial x_i} \right)_O = -\sum_n A_{n,i} p_n, \tag{13}$$

where $A_{n,i}$ is the i-direction component of the face area vector $\mathbf{A}_n$ in a Cartesian co-ordinate system and p_n is the fluid pressure on the face segment n of the circular cell on the axis. Thus, p_n may be computed based on the fluid pressure values stored at the centers of the cell on the axis and the cell next to the axis, i.e. at centers O and N in Figure 3, by using linear interpolation and this may be expressed as follows

$$p_n = f p_N + (1 - f) p_O, \tag{14}$$

where f is a weight function given by

$$f = r_n / r_N, \tag{15}$$

© 1998 John Wiley & Sons, Ltd.

where r_n is the radius of the circular cell. For a uniform grid we have $f = 0.5$.

For the unknown values of the fluid velocity, $u_{i,n}$, in the convection term on the face of the cell on the axis, see Equation (11), various interpolation schemes can be used. However, it was found that when using either the QUICK or the upwind schemes, it does not make a large difference with respect to the overall accuracy of the numerical results on the axis and therefore, in the results presented for these test examples, the simple upwind scheme has been employed to compute the fluid velocity, $u_{i,n}$, on the face of the cell on the axis and this may be expressed as

$$u_{i,n} = u_{i,\mathrm{O}} \quad \text{when} \quad F_n \geq 0 \tag{16}$$

and

$$u_{i,n} = u_{i,\mathrm{N}} \quad \text{when} \quad F_n < 0. \tag{17}$$

In a similar way to that used to produce Equation (5), Equation (11) may now be expressed in general form under the upwind scheme as follows

$$a_{\mathrm{O}} u_{i,\mathrm{O}} = \sum_n a_n u_{i,\mathrm{N}} - \sum_n f A_{n,i} p_{\mathrm{N}}, \tag{18}$$

where the subscript O is the center of the cell on the axis, and the a's are coefficients which are given by

$$a_n = D_n + [-F_n, 0] \quad \text{and} \quad a_{\mathrm{O}} = \sum_n a_n, \tag{19}$$

where the diffusion term D is given by

$$D_n = \mu \frac{A_n}{r_{\mathrm{N}}}. \tag{20}$$

The convection term F will be discussed in the next section.

It can be observed from Equation (18) that all the values of the fluid pressure around the cell on the axis have been taken into account in the momentum equation in order to produce a total pressure difference in the i-direction. However, the pressure on the axis does not play a role in the momentum Equation (18) and the computation of the pressure on the axis will be discussed later.

3.3. Flux of fluid through the face of the circular cell on the axis

The most crucial task which has to be faced in the treatment of the axis is the computation of the pressure on the axis. The reason for this is that an explicit governing equation for the fluid pressure is not available and normally we rely on the mass continuity equation to construct a pressure correction equation to compute the pressure. Therefore, the current pressure–velocity coupling method is very sensitive to any changes in the mass flux through the cell faces. In order to maintain consistency as much as possible in the whole computational domain, the same pressure–velocity coupling strategy to that which has been used for the fluid flow on a general cell is used to compute the pressure on the axis and thus a pressure correction equation on the axis has to be developed. Before a pressure correction equation from the continuity equation can be obtained, an equation to compute the mass flux of fluid through the face of the circular cell on the axis must first be obtained and have the pressure on the axis explicitly expressed in it. In order to do this, a set of supplementary rectangular

© 1998 John Wiley & Sons, Ltd.

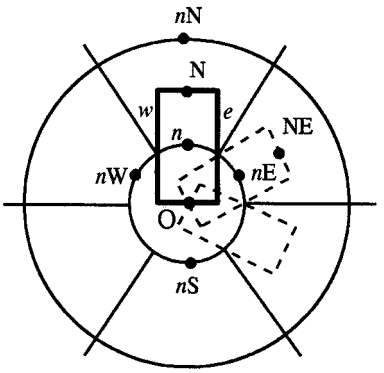

Figure 5. The control volumes used to compute the pressure correction on the axis of the polar cylindrical grid system.

cells around the axis was introduced, see Figure 5. The rectangular cells are designed to have their center located at the center of each face segment of the cell on the axis, so that the flux velocity vector **V** on the face segment of the circular cell on the axis may be computed by implementing the general discretized momentum Equation (5) on these rectangular cells as follows

$$a_n V_{i,n} = \sum_{nb} a_{nb} V_{i,nb} - \Omega \left(\frac{\partial p}{\partial x_i} \right)_n, \tag{21}$$

where $V_{i,n}$ is the flux velocity component of the fluid through the face of the circular cell on the axis, the subscript nb denotes the neighboring cells on the east (nE), west (nW), north (nN) and the south (nS) side of the rectangular cell, see Figure 5. On each of these neighboring cells, the fluid velocity $V_{i,nb}$ may be computed by interpolation based on the fluid velocities stored at the nearby cell centers. For example, on the north point nN we have

$$V_{i,n\mathrm{N}} = \frac{1}{2} (V_{i,\mathrm{N}} + V_{i,\mathrm{NN}}). \tag{22}$$

As far as the coefficients a are concerned, Equations (6)–(8) may still be implemented on the rectangular cell system to compute them. While computing the flux of the fluid, F_{nn}, the flux velocities of the fluid on the north face (N) and the south face (O) of the rectangular cell may take the values of the fluid velocity which have been stored there, whilst the values of fluid velocity on the east (e) and west (w) faces must be computed by using an interpolation scheme based on the values of the fluid velocities stored at the cell centers around it. For example, for a uniform grid on the east face we have

$$\mathbf{V}_e = \frac{1}{4} (\mathbf{V}_{\mathrm{NE}} + \mathbf{V}_{\mathrm{N}} + 2\mathbf{V}_{\mathrm{O}}). \tag{23}$$

The fluid pressure gradient source term in Equation (21) may be computed based on the values of the fluid pressure on the faces of the rectangular cells and by using the following equation

$$-\Omega \left(\frac{\partial p}{\partial x_i} \right)_{\mathrm{P}} = -[A_{\mathrm{N},i} p_{\mathrm{N}} - A_{\mathrm{O},i} p_{\mathrm{O}} + A_{e,i} p_e - A_{w,i} p_w]. \tag{24}$$

Again, the values of the fluid velocity for the convection on the east (e) and the west (w) faces must be computed by using an interpolation scheme. Bearing in mind that the aim is to

© 1998 John Wiley & Sons, Ltd.

compute the mass flux of fluid through the face of the circular cell on the axis, the pressure on the east and west faces of the rectangular faces are not very important as they mainly effect the tangential velocity of the fluid on the circular face.

It can be observed that by using Equation (24), the pressure on the axis of the cylindrical grid system, p_O, has been explicitly included in the momentum Equation (21) which can be used to compute the mass flux of fluid through the face of the circular cell on the axis, and this allows a pressure correction equation on the axis based on the continuity equation to be constructed.

3.4. Pressure correction equation on the axis

If we start from a guessed fluid pressure field, which is denoted p^*, then a guessed fluid velocity on the face of the cell on the axis can be obtained using Equation (21), which is denoted V_n^*. Supposing that an accurate solution for the fluid pressure, which is denoted p^{**}, can be obtained from the guessed value p^* plus a correction p' as follows

$$p^{**} = p^* + p'. \tag{25}$$

Then a corrected fluid velocity, V^{**}, can be obtained from Equation (21), and this can be expressed as

$$V_n^{**} = V_n^* + V_n'. \tag{26}$$

Now if the continuity Equation (2) is integrated over the circular control volume on the axis, this gives rise to

$$\sum_n \rho \mathbf{V}_n \cdot \mathbf{A}_n = 0, \tag{27}$$

and by substituting Equation (26) into Equation (27) we have

$$\sum_n \rho (\mathbf{V}_n* + \mathbf{V}_n') \cdot \mathbf{A}_n = 0, \tag{28}$$

where the superscripts * and $'$ denote the guessed and the corrected values, respectively, in the iterative process and the subscript n represents the value on the face of the control volume on the axis.

If we further employ the same procedure as that used to obtain the pressure correction equation in the SIMPLE algorithm [5], and introduce Equations (25) and (26) into Equation (21), and then substitute Equation (21) into the continuity Equation (27) and ignore the first term on the right hand side of Equation (21), for a uniform grid, the following pressure correction equation on the axis is obtained

$$a'_O p'_O = \sum_n a'_n p'_{i,N} - \sum_n \rho \mathbf{V}_n^* \cdot \mathbf{A}_n, \tag{29}$$

where the p'_O and $p'_{i,N}$ are the pressure correction for the fluid pressure on the axis and on the cell center N, see Figure 5, and the coefftcients a' are given by, respectively,

$$a'_0 = \sum_n a'_n \quad \text{and} \quad a'_n = \rho A_n^2 / a_n. \tag{30}$$

It is worth pointing out that the coefficient a_n in Equation (30) takes the value that is obtained from Equation (21), rather than the average of the coefficients a_p on the nearby cell centers as is used for the general polar cylindrical cells.

© 1998 John Wiley & Sons, Ltd.

4. SOLUTION STRATEGY

For a particular fluid flow problem in a polar cylindrical computational domain, in which the axis of the domain is included, Equations (5) and (9) can be used to compute the fluid velocity and the pressure on a general polar cylindrical cell which is not located on the axis and use Equations (18) and (29) to compute the fluid velocity and the pressure on the axis by an iterative procedure. If the cylindrical periodical boundary condition is enforced on a radial grid line, e.g. the grid line where $\theta = 0$, then the computational domain may be split from this grid line and form a rectangular domain in the computational space. Therefore, the commonly employed line-by-line iterative method may be used to solve the discretized momentum and the pressure correction equations on the computational domain. The cell on the axis may act as a boundary cell for the cells around it in the iteration process and the data on the axis may be up-dated on each iteration.

5. ILLUSTRATIVE EXAMPLES

To illustrate the effectiveness of the numerical treatment that has been adopted for dealing with the axis when a polar cylindrical grid system has been employed, two simple, two-dimensional fluid flows have been simulated and the results obtained are presented.

5.1. Fluid flow in a rotating circular cylinder

In order to check if the proposed new treatment of the axis works well in an axially symmetrical fluid flow situation, the solid body rotating fluid flow in a cylinder was simulated by the proposed method. As a boundary condition, a constant circumferential velocity, u_θ, was specified on the cylinder of given radius $r = r_0$ as follows

$$u_\theta = u_0 \quad \text{on} \quad r = r_0, \tag{31}$$

where u_0 is a constant.

Subject to the boundary condition (31), an axisymmetrical solid body rotating fluid flow will be produced inside the cylinder, i.e. the circumferential component of the fluid velocity is directly proportional to the radial distance to the axis and the radial component of the fluid velocity is zero everywhere in the cylinder. The fluid pressure inside the cylinder has a parabolic variation along the radial direction and the radial pressure gradient balances the centripetal acceleration of the fluid.

In order to numerically simulate this solid body rotating fluid flow with the axis of the cylinder being included in the computational domain, a polar cylindrical grid has been constructed with polar cylindrical cells being used in the regions which are not in the vicinity of the axis and a circular cell being employed on the axis. Three grid sizes, namely 10×20, 20×40 and 40×80, have been employed in the simulation and the grid lines are uniformly distributed, where the first and second integers of the grid sizes are the numbers of the grid lines used in the radial and the circumferential directions of the computational domain, respectively, and a uniform grid was used. Further, the Reynolds number, Re, of the fluid flow is defined by

$$Re = \rho u_0 d/\mu, \tag{32}$$

where ρ is the fluid density, μ is the fluid viscosity, d is the diameter of the cylinder and u_0 is

© 1998 John Wiley & Sons, Ltd.

the characteristic fluid velocity. In the simulation of this solid body rotating fluid flow, the u_0 value takes that of the circumferential velocity, u_θ , which is specified on the cylinder by the boundary condition (31) and the Reynolds number of the fluid flow is $Re = 100$.

Figure 6 illustrates the numerically obtained fluid velocity and the pressure as a function of the radial distance from the axis of the rotating cylinder and for a comparison, the analytical solution of a solid body rotating fluid flow is also presented. It can be observed that the numerically predicted fluid velocity and the pressure are in very good agreement with the analytical solution. As a matter of fact, when a grid size of 40×80 is used, the numerical results for the fluid velocity and pressure are virtually indistinguishable from the analytical solution and therefore, these results have not been presented in Figure 6.

5.2. Fluid flow in a two-dimensional channel

It is well known that the fully developed laminar fluid flow in a two-dimensional channel has a parabolic velocity profile across the channel and a streamwise linear variation in the pressure. In order to examine if the treatment of the axis works well when there is a strong flux of fluid across the axis, a fully developed fluid flow in a two-dimensional channel was simulated by using the proposed technique. The grid was generated such that the axis of the grid system was situated on the central plane of the channel, i.e. where the fluid flow takes its maximum velocity, see Figure 7, and a parabolic velocity profile, u, was specified as a boundary condition on the cylindrical boundary of the grid as

$$u = u_0[1 - (2y/b)^2] \quad \text{on} \quad r = r_0, \tag{33}$$

where y is the distance from the central plane of the channel, b is the height of the channel and the x-axis is along the length of the channel being measured positive in the direction of the fluid flow. The prediction of the fluid flow inside the cylindrical region was required.

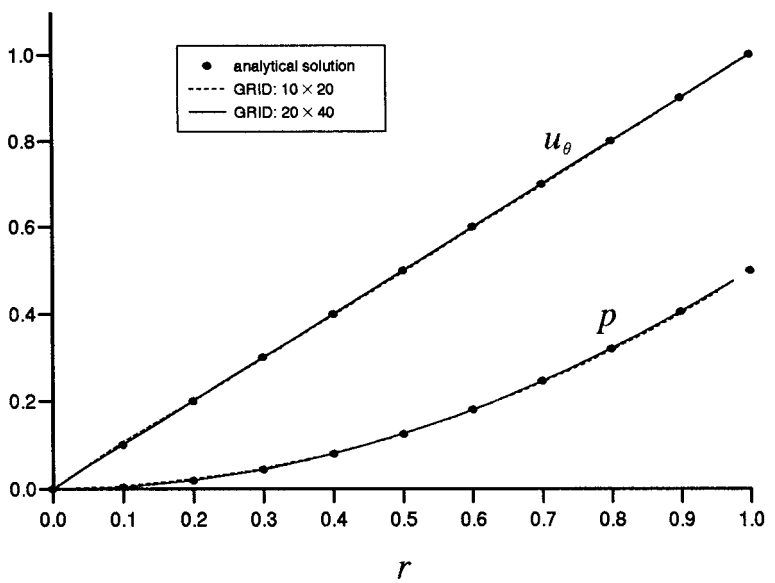

Figure 6. Comparison of the numerically obtained fluid velocity and pressure with the analytical solution for the solid body rotating fluid flow.

© 1998 John Wiley & Sons, Ltd.

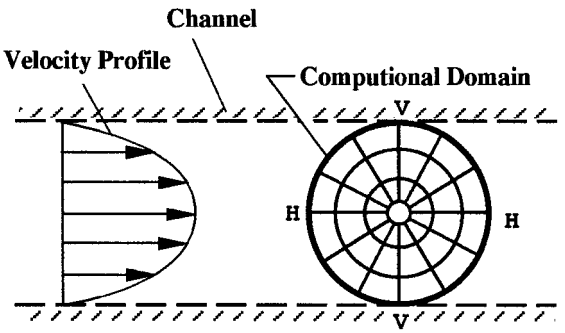

Figure 7. The computational domain used for simulating the fluid flow in a channel.

Results have been obtained for two Reynolds numbers, namely $Re = 1$ and $Re = 100$, using the same three grid sizes as those employed in the solid body rotating fluid flow simulations in Section 5.1. In this simulation, both the QUICK and the upwind scheme have been used.

In order to focus on the treatment of the axis, the numerically obtained fluid velocity and the pressure are compared with the analytical solution along the two lines which go across the axis of the grid, i.e. the vertical line V-V and the horizontal line H-H, see Figure 7.

Figure 8 shows the numerically derived fluid velocity for the channel flow along the vertical line V-V, see Figure 7, with $Re = 1$ and at various grid sizes. Also presented in Figure 8 is the analytical solution for the fluid velocity. It is observed that both the fluid velocity and the pressure obtained when using the upwind and the QUICK schemes are almost indistinguishable from each other at such low Reynolds number fluid flows. It can be observed from Figure 8 that the numerically obtained fluid velocity shows very good agreement with that of the analytical solution, even when using a very coarse grid of 10×20. As the grid used in the

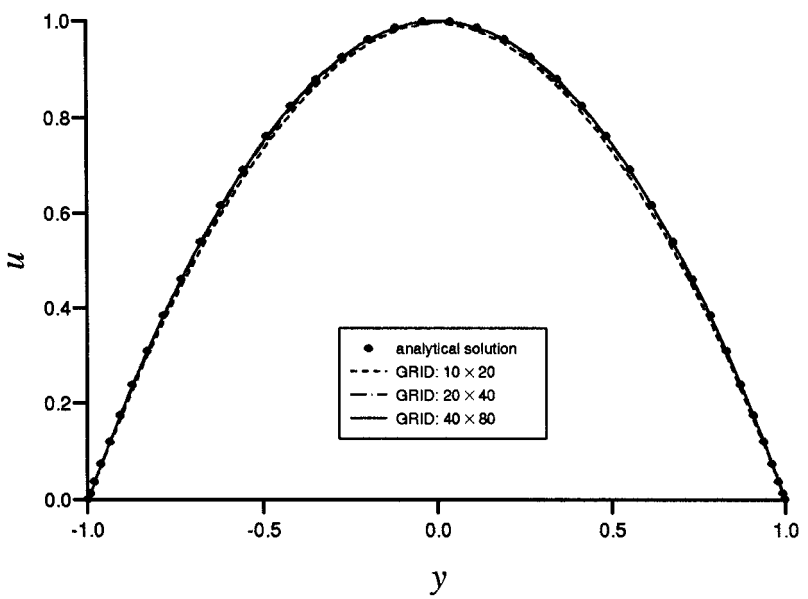

Figure 8. Comparison of the numerically obtained fluid flow velocity across the axis of the polar cylindrical grid in a two-dimensional channel for $Re = 1$.

© 1998 John Wiley & Sons, Ltd.

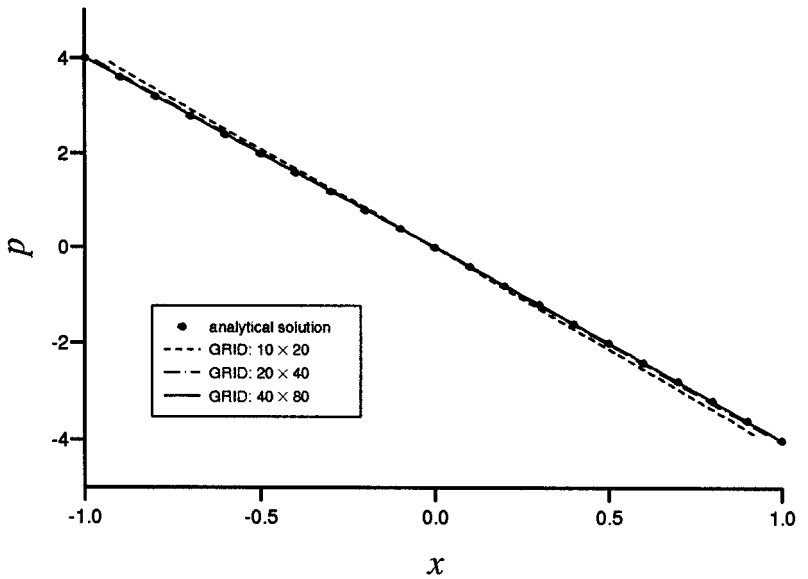

Figure 9. Comparison of the numerically obtained fluid flow pressure across the axis of the polar cylindrical grid in a two-dimensional channel for $Re = 1$.

simulation becomes finer, for example 20×40 or finer, the numerical results have been found to be almost indistinguishable from the analytical solutions.

Figure 9 shows the comparison of the simulated fluid pressure with the analytical solution along the horizontal line H-H, see Figure 7, for $Re = 1$. It can be observed from this figure that there is a very smooth profile for the fluid pressure across the axis for all the three grid sizes investigated in the simulation. When compared with the analytical solution for the fluid pressure, it has been found that there is good agreement between the numerical and the analytical solutions when a reasonably fine grid is employed, for example 20×40.

Figures 8 and 9 illustrate that the treatment of the axis works well when using both the first-order upwind scheme and the second-order QUICK scheme for low Reynolds number fluid flows, say Re is O(1). We now investigate fluid flows at larger Reynolds number, e.g. $Re = 100$, and use the same three grid sizes and both the upwind and the QUICK schemes to those which we used for the simulations of the low Reynolds number fluid flows.

Figures 10 and 11 are the results obtained for the fluid velocity and the pressure along the lines V-V and line H-H, respectively, see Figure 7, when using the upwind scheme for the Reynolds number of the fluid flow $Re = 100$. It is observed that there is a deterioration in the numerically obtained fluid velocity and the pressure, especially the pressure results which become worse in almost all of the computational domain, when compared with the corresponding results which we obtained in the low Reynolds number case as illustrated in Figures 8 and 9. The results become even less accurate when using a coarse grid, e.g. 10×20, but it can also be observed that the accuracy of the numerical results can be improved when using a finer grid. The reason for this is due to the effect of the artificial viscosity which is introduced by the upwind scheme and this effect increases as the Reynolds number of the fluid flow increases.

© 1998 John Wiley & Sons, Ltd.

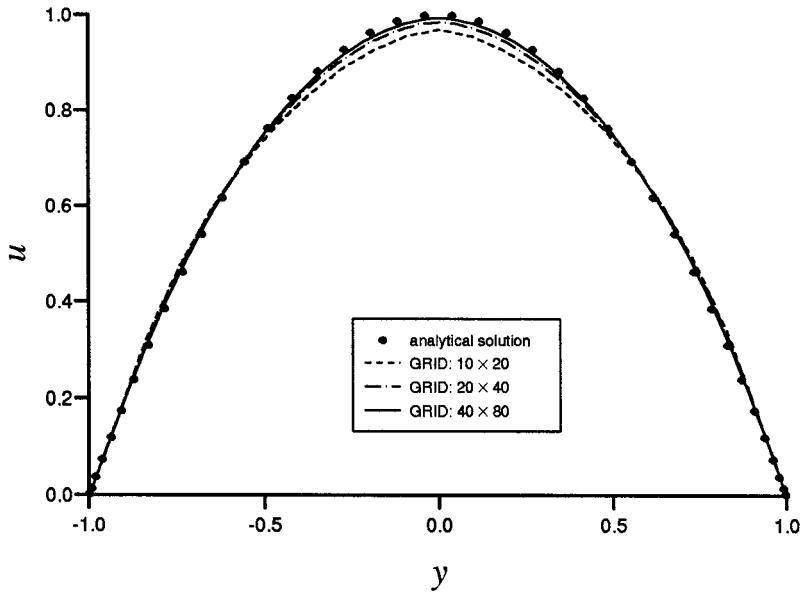

Figure 10. Comparison of the numerically obtained fluid flow velocity across the axis of the polar cylindrical grid in a two-dimensional channel with $Re = 100$ when using the upwind scheme.

In order to reduce the affect of the artificial viscosity, the QUICK scheme has been used and the numerical results obtained are shown in Figures 12 and 13 for $Re = 100$. Figure 12 shows the fluid velocity along the line V-V, see Figure 7, and Figure 13 shows the pressure distribution alone the line H-H, see Figure 7. Under the QUICK scheme a substantial

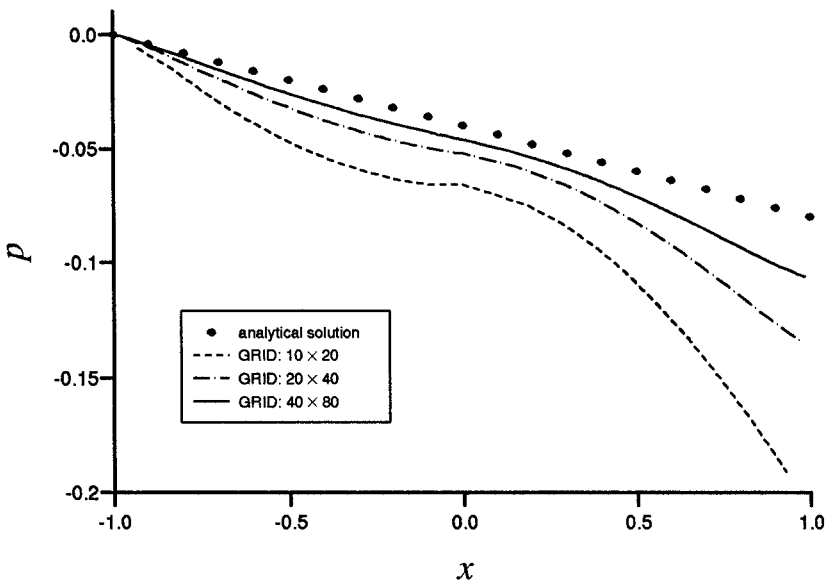

Figure 11. Comparison of the numerically obtained fluid flow pressure across the axis of the polar cylindrical grid in a two-dimensional channel with $Re = 100$ when using the upwind scheme.

© 1998 John Wiley & Sons, Ltd.

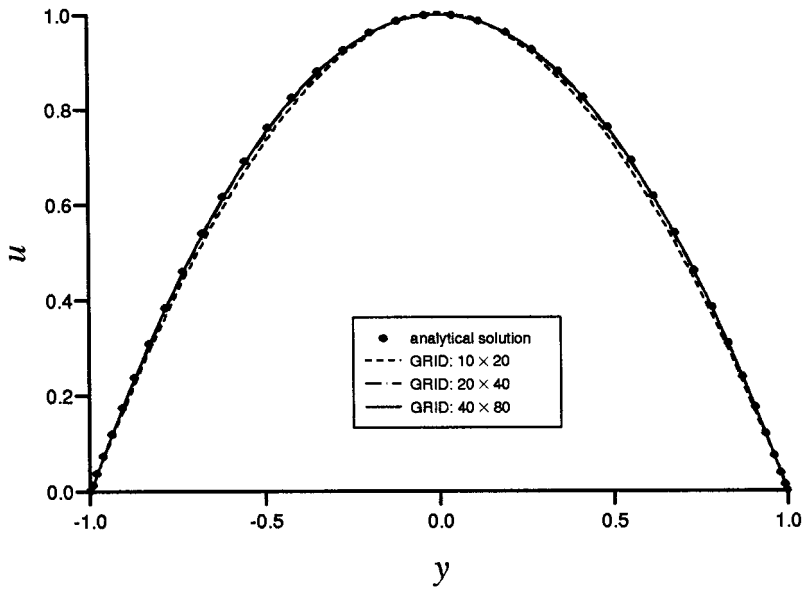

Figure 12. Comparison of the numerically obtained fluid flow velocity across the axis of the polar cylindrical grid in a two-dimensional channel with $Re = 100$ when using the QUICK scheme.

improvement in the numerically obtained fluid velocity and the pressure are obtained when compared with the analytical solution to the fluid flow. Again, we obtained a very smooth fluid velocity and pressure variations across the axis and the results are in good agreement with the analytical results when a reasonably fine grid, for example 20×40, is employed.

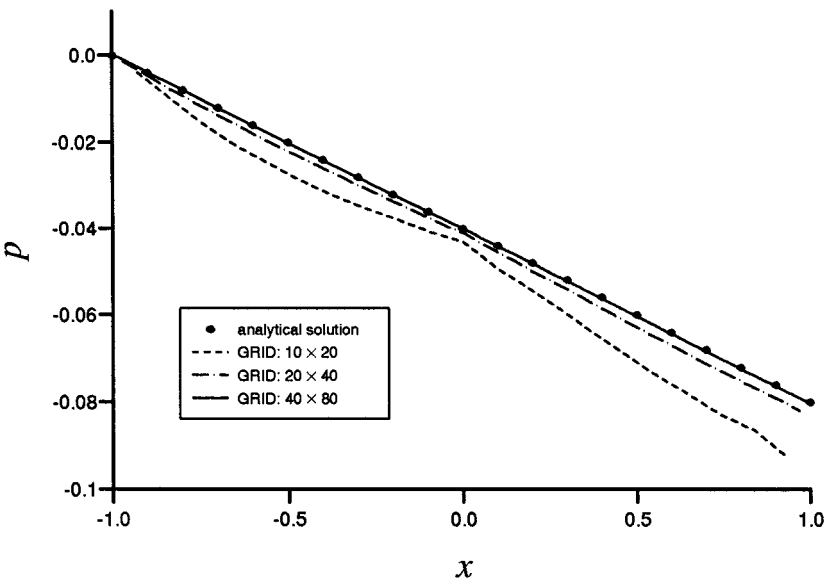

Figure 13. Comparison of the numerically obtained fluid flow pressure across the axis of the polar cylindrical grid in a two-dimensional channel with $Re = 100$ when using the QUICK scheme.

© 1998 John Wiley & Sons, Ltd.

6. REMARKS AND CONCLUSIONS

In this paper a special circular control volume has been introduced on the axis of a polar cylindrical grid system in order to deal with the difficulty that occurs when the control volume cells around the axis degenerate from being general quadrilaterals to triangles. Then a control volume method was developed using this circular cell on the axis and a non-staggered grid arrangement. The method has been shown to give good numerical simulations to the fluid flows in a polar cylindrical grid system where the axis has been included in the computational domain.

The extension of this new method to the more general three-dimensional case is straightforward. In this situation a cylindrical control volume may be used on the axis of the polar cylindrical grid system and the governing equations may be expanded into a three-dimensional form in a general manner.

ACKNOWLEDGMENTS

The authors would like to thank the COLT Foundation for some of the financial support of this work.

REFERENCES

1. S.V. Patankar, V.S. Pratap and D.B. Spalding, 'Prediction of laminar flow and heat transfer in helically coiled pipes', *J. Fluid Mech.*, **62**, 539–551 (1974).
2. C. Hirsch, *Numerical Computation of Internal and External Flows*, Wiley, London, 1988.
3. R. Verzicco and P. Orlandi, 'A finite-difference scheme for three-dimensional incompressible flows in cylindrical co-ordinates' *J. Comput. Phys.*, **123**, 402–414 (1996).
4. J.G.M. Eggels, *Ph.D. Thesis*, Delft University of Technology, Delft, Netherlands, 1994
5. S.V. Patankar, *Numerical Heat Transfer and Fluid Flow*, Hemisphere, Washington DC, 1980.
6. C.M. Rhie and W.L. Chow, 'Numerical study of the turbulent flow past an airfoil with trailing edge separation', *AIAA J.*, **21**, 1525–1532 (1983).
7. B.P. Leonard, 'A stable and accurate convective modelling procedure based on quadratic upstream interpolation', *Comp. Methods Appl. Mech. Eng.*, **19**, 59–98 (1979).

© 1998 John Wiley & Sons, Ltd.